Ultrasonics 91 (2019) 30–33

Contents lists available at ScienceDirect

Ultrasonics

journal homepage: www.elsevier.com/locate/ultras

Method of the out-of-band rejection improvement of the AlN based surface acoustic wave filters

Shuai Yang[a,b], Yujie Ai[a,b,*], Zhe Cheng[a,b], Lian Zhang[a,b], Lifang Jia[a,b], Boyu Dong[c], Baohui Zhang[c], Junxi Wang[a,b], Yun Zhang[a,b,*]

[a] Institute of Semiconductors, Chinese Academy of Sciences, Beijing 100083, China
[b] University of Chinese Academy of Sciences, Beijing 100049, China
[c] NAURA Technology Group Co., Ltd., Beijing 100176, China

ARTICLE INFO

Keywords:
AlN films
High acoustic propagation velocity
Surface acoustic wave filters
Delay gap
Out-of-band rejection improvement

ABSTRACT

AlN based surface acoustic wave (SAW) filters with an acoustic wavelength (λ) of 8 μm have been fabricated based on sputtered AlN films on sapphire. The acoustic velocity of 1-μm-AlN/Sapphire bilayer structure is 5536 m/s, 60% higher than that of $LiNbO_3$. The central frequency, insertion loss, out-of-band rejection, and bandwidth of fabricated AlN based two-port type SAW filters with a delay gap of λ are 692 MHz, 25.58 dB, 35.40 dB, and 2.7 MHz, respectively. The impact of delay gap on the performance of AlN based filters have been studied experimentally. By the analysis of frequency response of SAW filters with delay gaps of λ, 15λ, and 30λ with and without time gating technique, we find that increase the delay gap of AlN based SAW resonators can improve the out-of-band rejection effectively because of the reduction of electromagnetic coupling, with a cost of a little degradation of insertion loss due to the small propagation loss of AlN/Sapphire bilayer. When the delay gap is increased from λ to 15λ, out-of-band rejection of AlN based filters is increased by 4.75 dB, while the insertion loss is only increased by 0.81 dB. When the delay gap is further increased from 15λ to 30λ, the suppression of out-of-band rejection is not obvious.

1. Introduction

Surface acoustic wave (SAW) devices have attracted increasing attention due to their widely applications in mobile communications as well as various kinds of sensors [1–7]. Bulk piezoelectric substrates, such as $LiNbO_3$, and $LiTaO_3$, are the most widely used materials for SAW resonators and filters in front-end radio frequency modules for mobile communications. However, the working frequency of most SAW devices based on these traditional piezoelectric materials is below 3 GHz, which can't meet the increasing demand of high working frequency from advanced mobile communication systems [8]. Usually, operating frequency of SAW device can be increased by introducing smaller interdigital transducer (IDT) fingers width or piezoelectric substrates with higher acoustic velocity. However, reducing the width of IDT fingers will propose a great challenge for photolithography. Moreover, the quality factor and power handling capability of SAW resonators degrades severely with the reduction of width of IDT fingers [9]. As a result, AlN based SAW devices on sapphire have attracted much attention for high frequency applications due to its high acoustic propagation velocity (more than 5500 m/s) and low acoustic propagation loss [10,11].

A well-performing AlN based SAW filters are required to exhibit a small insertion loss, a large out-of-band rejection, and usually a wide bandwidth [12]. The insertion loss of AlN based resonator can be reduced by improving crystal quality of AlN films [13,14], and the bandwidth of filters can be tuned by the doping of AlN films [15,16]. The out-of-band rejection of AlN based SAW resonators and filters is mainly influenced by substrate, because the background noise of SAW devices is determined by the electromagnetic coupling between the input and output IDTs of SAW devices. For example, I. Ingrosso, et al. have reported that the out-of-band rejection of AlN based SAW filters on Si can be increased by the increase of substrate resistivity [17]. They also have reported that the out-of-band rejection of AlN based SAW filters on Si can be improved by 30 dB by inserting a Si_3N_4 interlayer between Si and AlN films, however, the insertion loss shows severely degradation, which is more than 30 dB [17]. Except the impact of substrate, little work has been done focusing on out-of-band rejection capability improvement for AlN based SAW filters. Very recently, Junning Gao, et al. have reported that the out-of-band rejection of two-port type AlN based SAW filters can be improved by increasing the

* Corresponding authors at: Institute of Semiconductors, Chinese Academy of Sciences, Beijing 100083, China.
E-mail addresses: aiyujie@semi.ac.cn (Y. Ai), yzhang34@semi.ac.cn (Y. Zhang).

https://doi.org/10.1016/j.ultras.2018.07.008
Received 30 January 2018; Received in revised form 26 June 2018; Accepted 16 July 2018
Available online 17 July 2018
0041-624X/

number of IDT fingers, however, the bandwidth were reduced sharply with the increase of number of IDT fingers [18].

In this paper, we try to improve the out-of-band rejection of AlN based SAW filters by increasing the distance between input and output IDTs (delay gap), because we think that the electromagnetic coupling between input and output IDTs of SAW filters will be reduced with the increase of delay gap. However, with the increase of delay gap, the insertion loss of SAW resonators will also be increased due to the propagation loss increment. As a result, with the increase of delay gap, out-of-band rejection will be improved while insertion loss will be degraded, however, which one is dominant for AlN based SAW filters is unknown. In this paper we study the impact of delay gap on insertion loss, out-of-band rejection and bandwidth of AlN based SAW filters systematically, which may be meaningful for the design of high performance AlN based SAW filters for communication or sensor applications.

2. Experimental details

AlN films with thickness of 1 μm were deposited on 2 inch sapphire wafers by RF reactive sputtering with a high purity Al target in Ar and N_2 gas mixture at 650 °C. Then, two-port type Rayleigh wave SAW filters with Ti/Al electrodes (10 nm/150 nm) were fabricated by electron beam evaporation and lift-off photolithography process. The SAW filters on AlN/Sapphire bilayer include an input IDTs, an output IDTs and a pair of reflectors, as shown in Fig. 1(a). For comparison, two-port type SAW filters on a 64° Y-Z cut bulk $LiNbO_3$ substrate were also fabricated with the same fabrication process. Fig. 1(b) shows the magnified microscope of IDTs. The IDTs contains 100 pairs of equal-interval-finger electrodes with a width of 2 μm and a metallization ratio of 50%, corresponding to an acoustic wavelength (λ) of 8 μm. The acoustic aperture of the IDT fingers is 30λ. Each reflector contains 100 short-circuited gratings. To investigate the impact of the distance between input IDTs and output IDTs (delay gap) on the performance of AlN based SAW filters, SAW filters with different delay gaps of λ, 15λ and 30λ have been fabricated, and we refer to them as sample A, sample B and sample C, respectively.

The crystal quality and surface morphology of sputtered AlN films are characterized by high resolution X-ray diffraction (HRXRD, Bede D1) and atomic force microscopy (AFM, Veeco D3100), respectively. The RF characteristics of SAW devices were measured by network analyzer (Rohde & Schwarz ZVB8) with a standard calibration method.

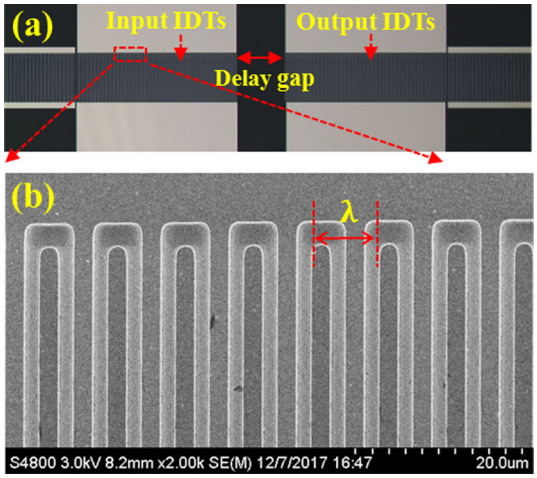

Fig. 1. Microscope of (a) two-port type AlN based SAW filter, and (b) magnified picture of IDT fingers.

3. Results and discussion

Fig. 2(a) shows the 2θ-ω XRD scan pattern of sputtered AlN films on sapphire. The diffraction peaks at 2θ = 36.1°, and 41.8° correspond to the (0002) plane of AlN phase with hexagonal structure and the (0006) plane of sapphire, which means a highly c-axis textured AlN thin film was successfully grown on the sapphire substrates. The inset of Fig. 2(a) shows the XRD rocking curve of AlN films, indicating that the full width at half maximum (FWHM) value of AlN films is as low as 0.2°. In fact, a low FWHM of AlN films is very important to fabricate SAW devices with better electric properties [19]. The surface morphology of AlN films was characterized using AFM. As shown in Fig. 2(b), the AFM image of AlN films reveals a homogeneous surface without abnormally grown grains. The root mean square (rms) roughness value of AlN film is 1.37 nm in a range of 10 × 10 μm. The low surface roughness of AlN films is helpful to reduce the propagation loss of SAW filters [20].

Fig. 3 shows the measured frequency responses (S_{21}) of sample A. For comparison, the inset in Fig. 3 shows the S_{21} of $LiNbO_3$ based SAW filters with the same λ of 8 μm. The central frequency (f_c) of sample A and $LiNbO_3$ based SAW filters are 692 MHz and 427 MHz, respectively. The velocity of Rayleigh wave (v_{SAW}) can be calculated according to Eq. (1) [21]

$$v_{SAW} = \lambda \cdot f_c \tag{1}$$

where f_c is the central frequency and λ is the acoustic wavelength of SAW devices, which gives 5536 m/s for AlN/Sapphire bilayer structure, and 3416 m/s for $LiNbO_3$ bulk substrate. The results indicate that the v_{SAW} of AlN/Sapphire structure can be increased by 60% than that of $LiNbO_3$. The insertion loss of sample A is defined as the insertion loss at f_c, the out-of-band rejection is calculated by the average out-of-band rejections from 670 MHz to 680 MHz, and the bandwidth is a 3-dB bandwidth with the insertion loss of f_c as a reference. As shown in Fig. 3, the insertion loss, out-of-band rejection, and bandwidth of Sample A are 25.58 dB, 35.40 dB, and 2.7 MHz, respectively.

Fig. 4(a) shows the frequency response (S_{21}) of the SAW filters with different delay gaps between input and output IDTs without time gating technique. The delay gap of sample A, sample B and C are λ, 15λ, and 30λ, yielding a distance of 8 μm, 120 μm, and 240 μm, respectively. All the three samples exhibit an obvious typical filter performance with a central frequency around 692 MHz. The f_c, insertion loss, out-of-band rejection, and bandwidth of the three samples are listed in Table 1. As shown in Table 1, when the delay gap is increased from λ to 15λ, the out-of-band rejection of AlN based filters are increased greatly from 35.40 dB to 40.15 dB, showing a 4.75 dB improvement, while the insertion loss is only increased by 0.81 dB, from 25.58 dB to 26.39 dB. The out-of-band rejection of AlN based filters increase a little from 40.15 dB to 40.71 dB when the delay gap is further increased from 15λ to 30λ.The out-of-band rejection improvement may be attributed to a reduced electromagnetic coupling between input and output IDTs of SAW filters [22], and the insertion loss degradation is resulted from the increase of propagation loss with the increase of delay gap from λ to 15λ. The propagation loss (α) of Rayleigh wave on the AlN/Sapphire bilayer calculated by Eq. (2) [23] is 0.057 dB/λ.

$$\alpha = \frac{IL_B - IL_A}{Gap_B - Gap_A} \tag{2}$$

where IL_A and IL_B are the insertion losses of sample A and B, Gap_A and Gap_B are the delay gaps of sample A and B, respectively. The bandwidths of sample A, B, and C are 2.7 MHz, 2.6 MHz, 2.4 MHz, respectively, indicating a small bandwidth reduction with the increase of delay gap.

In order to obtain an ideal frequency response spectrum of SAW filters with different delay gaps, it is necessary to eliminate the effect of electromagnetic coupling between the input and output electrodes by using the time gating technique [24,25]. Time gate goes from 20 to 6000 ns. Fig. 4(b) exhibits the frequency response (S_{21}) of the SAW

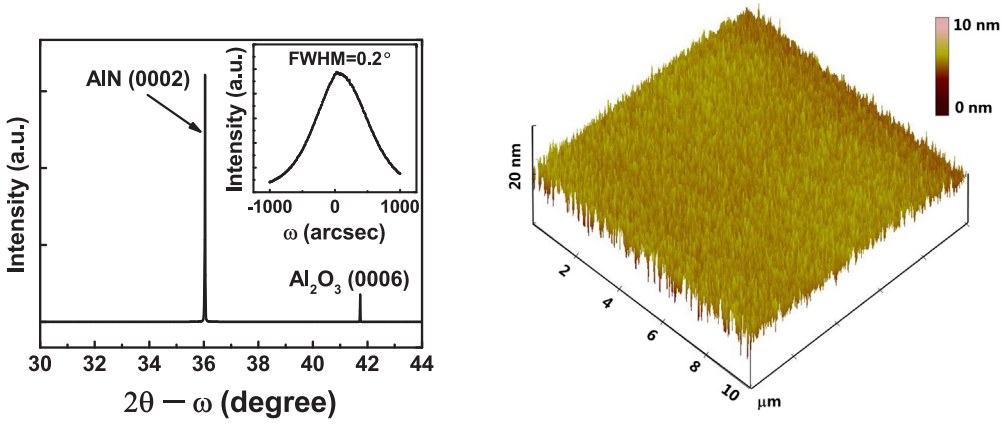

(a) (b)

Fig. 2. (a) The 2θ − ω XRD scan pattern of AlN thin films, and the inset shows the XRD rocking curve of AlN films. (b) 3D AFM image of AlN films in a range of 10 × 10 μm.

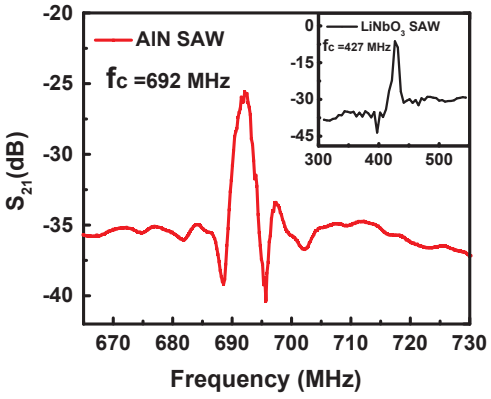

Fig. 3. Frequency response (S_{21}) of Sample A, and the inset shows the S_{21} of $LiNbO_3$ based SAW filters.

filters with time gating. The f_c, insertion loss, out-of-band rejection, and bandwidth of the three samples with time gating are listed in Table 1. Compared with the data without time gating, the three samples with time gating still exhibit similar f_c around 692 MHz. With time gating, the insertion loss of sample A, sample B, and sample C are increased from 25.58 dB, 26.39 dB, and 26.65 dB, to 28.01 dB, 28.14 dB, and 28.21 dB, exhibiting a 2.43 dB, 1.75 dB and 1.56 dB degradation, respectively. The insertion loss degradation can be attributed to the reduction of electromagnetic coupling at the resonant frequency with

Table 1
Measured SAW filters characteristics with different delay gaps.

	Without time-gating			With time-gating		
Delay gap	λ	15λ	30λ	λ	15λ	30λ
Central frequency (MHz)	692.1	692.8	692.7	692.5	692.7	692.7
Insertion loss (dB)	25.58	26.39	26.65	28.01	28.14	28.21
Out-of-band rejection (dB)	35.40	40.15	40.71	47.11	50.22	50.27
3-dB bandwidth (MHz)	2.7	2.6	2.4	3.2	3.5	3.4

time gating. The electromagnetic coupling of sample A is larger than that of sample B and C due to its smallest delay gap, as a result, sample A exhibits the largest insertion loss degradation. With time gating, the propagation loss (α) of Rayleigh wave on the AlN/Sapphire bilayer calculated by Eq. (2) is 0.009 dB/λ. This indicate that the propagation loss of AlN based SAW filters is overestimated without time gating due to the impact of electromagnetic coupling between input and output IDTs. With time gating, the out-of-band rejection of sample A, sample B, and sample C are increased from 35.40 dB, 40.15 dB, and 40.71 dB, to 47.11 dB, 50.22 dB, and 50.27 dB, exhibiting a 11.71 dB, 10.07 dB and 9.56 dB improvement, respectively. Because electromagnetic coupling of sample A is the largest among the three samples, therefore, sample A exhibits the largest out-of-band rejection improvement with time gating. Finally, we find that with time gating the 3-dB bandwidth of sample A, sample B, and sample C are increased from 2.7 MHz, 2.6 MHz, and 2.4 MHz, to 3.2 MHz, 3.5 MHz, and 3.4 MHz, respectively,

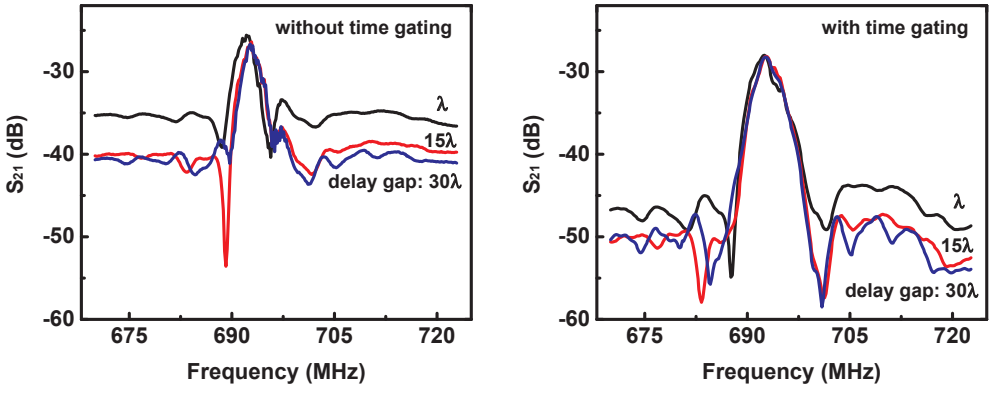

(a) (b)

Fig. 4. Frequency response (S_{21}) of AlN based SAW filters with different delay gaps (a) without time gating and (b) with time gating.

due to the reduction parasitic capacitor effect introduced by electromagnetic coupling.

Compare the frequency response of AlN based SAW filters with and without time gating, we find that for AlN based SAW filters, when the delay gap is increased, insertion loss will be degraded due to the increase of propagation loss, and out-of-band rejection will be improved due to more energy can be transferred through the acoustic path rather than electromagnetic coupling. The experimental results indicate that within 15λ, the improvement of out-of-band rejection will be dominant. Moreover, the insertion loss degradation with the increase of delay gap can be further suppressed by the reduction of propagation loss, which can be effectively attenuated with the improvement of crystal quality and surface roughness [26].

4. Conclusion

In conclusion, highly c axis-oriented AlN films with a FWHM value of XRD rocking curve for AlN (0002) plane of 0.2° and a roughness of 1.37 nm were prepared by RF reactive sputtering, and two-port type Rayleigh wave SAW filters based on AlN/Sapphire structure were fabricated by lift-off photolithography technique. The acoustic velocity and propagation loss of 1-μm-AlN/Sapphire bilayer structure are 5536 m/s and 0.057 dB/λ, respectively. We have systematically studied the impact of delay gap on the performance AlN based SAW filters. With the increase of delay gap from λ to 15λ, the out-of-band rejection is greatly increased by 4.75 dB and the insertion loss is increased a little by 0.81 dB. When the delay gap is increased from 15λ to 30λ, the out-of-band rejection almost does not change. Moreover, the impact of electromagnetic coupling on the performance of device is studied by time gating technique. With time gating, we find that the out-of-band rejection of sample A, sample B, and sample C are increased by 11.71 dB, 10.07 dB and 9.56 dB, respectively. Based on the experimental results with and without time gating, we find that increase the delay gap of AlN based resonators can improve the out-of-band rejection effectively because of the reduction of electromagnetic coupling, with a cost of a little degradation of insertion loss due to the small propagation loss of AlN/Sapphire bilayer.

Acknowledgements

This work was supported by the National Key Research and Development Program of China (Grant Nos. 2017YFB0402900), the National Natural Sciences Foundation of China (Grant Nos. 61604147 and 61674143), the One hundred person project of the Chinese Academy of Science.

References

[1] R. Takpara, M. Duquennoy, M. Ouaftouh, C. Courtois, F. Jenot, M. Rguiti, Optimization of PZT ceramic IDT sensors for health monitoring of structures, Ultrasonics 79 (2017) 96–104.
[2] B. Liu, X. Chen, H. Cai, M. Mohammad Ali, X. Tian, L. Tao, Y. Yang, T. Ren, Surface acoustic wave devices for sensor applications, J. Semicond. 37 (2016) 021001.
[3] S. Fujii, High-frequency surface acoustic wave filter based on diamond thin film, Physica Status Solidi (a) 208 (2011) 1072–1077.
[4] L. Perez-Cortes, C. Hernandez-Rodriguez, T. Mazingue, M. Lomello-Tafin, Functionality of Surface Acoustic Wave (SAW) transducer for palladium-platinum-based hydrogen sensor, Sensors Actuat. A-Phys. 251 (2016) 35–41.
[5] X.-G. Tian, H. Liu, L.-Q. Tao, Y. Yang, H. Jiang, T.-L. Ren, High-resolution, high-linearity temperature sensor using surface acoustic wave device based on $LiNbO_3$/SiO_2/Si substrate, Aip Adv. 6 (2016).
[6] E. Dogheche, D. Remiens, S. Shikata, A. Hachigo, High-frequency surface acoustic wave devices based on $LiNbO_3$/diamond multilayered structure, Appl. Phys. Lett. 87 (2005) 3351.
[7] S. Chen, Y. Zhang, S. Lin, Z. Fu, Study on the electromechanical coupling coefficient of Rayleigh-type surface acoustic waves in semi-infinite piezoelectrics/non-piezoelectrics superlattices, Ultrasonics 54 (2014) 604–608.
[8] A. Stefanescu, A. Müller, I. Giangu, A. Dinescu, G. Konstantinidis, Influence of Au-based metallization on the phase velocity of GaN on Si surface acoustic wave resonators, IEEE Electron. Device Lett. 37 (2016) 321–324.
[9] A. Reinhardt, L. Benaissa, J.B. David, N. Lamard, V. Kovacova, N. Boudou, E. Defaÿ, Acoustic filters based on thin single crystal $LiNbO_3$ films: Status and prospects, Proc. IEEE Ultrason. Symp. (2014) 773–781.
[10] G. Bu, D. Ciplys, M. Shur, L.J. Schowalter, S. Schujman, R. Gaska, Surface acoustic wave velocity in single-crystal AlN substrates, IEEE Trans. Ultrason. Ferroelectr. Freq. Control 53 (2006) 251–254.
[11] Y. Takagaki, T. Hesjedal, O. Brandt, K.H. Ploog, Surface-acoustic-wave transducers for the extremely-high-frequency range using AlN/SiC(0001), Semicond. Sci. Technol. 19 (2004) 256.
[12] X. Lu, K. Mouthaan, Y.T. Soon, Wideband bandpass filters with SAW-filter-like selectivity using chip SAW resonators, IEEE Trans. Microw. Theory Tech. 62 (2014) 28–36.
[13] B. Fu, F. Wang, R. Cao, Y. Han, Y. Miao, Y. Feng, F. Xiao, K. Zhang, Optimization of the annealing process and nanoscale piezoelectric properties of (002) AlN thin films, J. Mater. Sci.: Mater. Electron. (2017) 1–6.
[14] S. Fu, Q. Li, S. Gao, G. Wang, F. Zeng, F. Pan, Quality-enhanced AlN epitaxial films grown on c-sapphire using ZnO buffer layer for SAW applications, Appl. Surf. Sci. (2017).
[15] A. Kochhar, Y. Yamamoto, A. Teshigahara, K.y. Hashimoto, S. Tanaka, M. Esashi, Wave propagation direction and *c*-axis tilt angle influence on the performance of ScAlN/Sapphire-based SAW devices, IEEE Trans. Ultrason. Ferroelectr. Freq. Control 63 (2016) 953–960.
[16] W. Wang, P.M. Mayrhofer, X. He, M. Gillinger, Z. Ye, X. Wang, A. Bittner, U. Schmid, J.K. Luo, High performance AlScN thin film based surface acoustic wave devices with large electromechanical coupling coefficient, Appl. Phys. Lett. 105 (2014) 133502.
[17] I. Ingrosso, S. Petroni, D. Altamura, M. De Vittorio, C. Combi, A. Passaseo, Fabrication of AlN/Si SAW delay lines with very low RF signal noise, Microelectron. Eng. 84 (2007) 1320–1324.
[18] J. Gao, Z. Hao, E. Yanxiong, L. Niu, L. Wang, C. Sun, B. Xiong, Y. Han, J. Wang, H. Li, Surface acoustic wave devices fabricated on epitaxial AlN film, Funct. Mater. Lett. 09 (2016).
[19] U.C. Kaletta, P.V. Santos, D. Wolansky, A. Scheit, M. Fraschke, C. Wipf, P. Zaumseil, C. Wenger, Monolithic integrated SAW filter based on AlN for high-frequency applications, Semicond. Sci. Technol. 28 (2013) 065013.
[20] C. Li, X. Liu, L. Shu, Y. Li, AlN-based surface acoustic wave resonators for temperature sensing applications, Mater. Express 5 (2015) 367–370.
[21] B. Liu, M.A. Mohammad, D.-Y. Wang, X.-G. Tian, L.-Q. Tao, Y. Yang, T.-L. Ren, A comparison of Pd and Au electrodes-based LiNbO3 surface acoustic wave devices, Mod. Phys. Lett. B 30 (2016).
[22] K. Udo Ch, V.S. Paulo, W. Dirk, S. Alexander, F. Mirko, W. Christian, Z. Peter, W. Christian, Monolithic integrated SAW filter based on AlN for high-frequency applications, Semicond. Sci. Technol. 28 (2013) 065013.
[23] E. Blampain, O. Elmazria, T. Aubert, B.M. Assouar, O. Legrani, AlN/Sapphire: promising structure for high temperature and high frequency SAW devices, IEEE Sens. J. 13 (2013) 4607–4612.
[24] M. Clement, L. Vergara, J. Sangrador, E. Iborra, A. Sanz-Hervás, SAW characteristics of AlN films sputtered on silicon substrates, Ultrasonics 42 (2004) 403–407.
[25] U.C. Kaletta, C. Wipf, M. Fraschke, D. Wolansky, M.A. Schubert, T. Schroeder, C. Wenger, AlN/SiO_2/Si_3N_4/Si(100)-based CMOS compatible surface acoustic wave filter with −12.8-dB minimum insertion loss, IEEE Trans. Electron Devices 62 (2015) 764–768.
[26] K. Uehara, C.M. Yang, T. Shibata, S.K. Kim, S. Kameda, H. Nakase, K. Tsubouchi, Fabrication of 5-GHz-band SAW filter with atomically-flat-surface AlN on sapphire, Proc. IEEE Ultrason. Symp. (2004) 203–206.